

Supporting information for:

Reorientation of π -conjugated molecules on few-layer MoS₂ films

Jakub Hagara,[†] Nada Mrkyvkova,^{†,&,*} Peter Nádaždy,[†] Martin Hodas,[‡] Michal Bodík,[†]
Matej Jergel,[†] Eva Majková,^{†,&} Kamil Tokár,^{†,#} Peter Hutár,[§] Michaela Sojková,[§]
Andrei Chumakov,[‡] Oleg Konovalov,[‡] Pallavi Pandit,[‡] Stephan Roth,[‡] Alexander Hinderhofer,[‡]
Martin Hulman,[§] Peter Siffalovic^{†,&} and Frank Schreiber[‡]

[†]*Institute of Physics, Slovak Academy of Sciences, Dúbravská cesta 9, 845 11 Bratislava, Slovakia*

[&]*Center for Advanced Materials Application, Dúbravská cesta 9, Bratislava 84511, Slovakia*

[‡]*Institute of Applied Physics, University of Tübingen, Auf der Morgenstelle 10, D-72076 Tübingen, Germany*

[#]*Advanced Technologies Research Institute, Faculty of Materials Science and Technology in Trnava, Slovak University of Technology in Bratislava, 917 24 Trnava, Slovakia*

[§]*Institute of Electrical Engineering, Slovak Academy of Sciences, Dúbravská cesta 9, 845 11 Bratislava, Slovakia*

[‡]*European Synchrotron Radiation Facility, 71 avenue des Martyrs, Grenoble 38000, France*

[‡]*Photon Science, Deutsches Elektronen-Synchrotron (DESY), Hamburg 22607, Germany*

**Corresponding author: nada.mrkyvkova@savba.sk*

CONTENT

1. Experimental GIWAXS setup
2. As-measured absorption spectra
3. Raman spectra

References

1. *Experimental GIWAXS setup*

Scattering geometry for the real-time study of DIP growth is shown in Fig. S1. The angle of incidence (α_i) was set to 0.2° . The $\text{MoS}_2/\text{Al}_2\text{O}_3$ substrate and the crucible with DIP molecules were placed in the portable deposition chamber¹ with 360° cylindrical beryllium window which is transparent for X-rays.

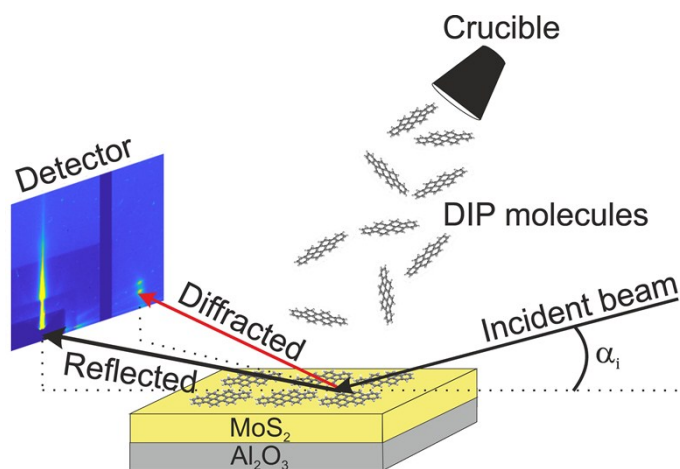


Figure S1. Schematic view of the in-situ GIWAXS measurement.

2. *As-measured absorption spectra*

The optical absorption data were measured ex-situ for DIP thin films with different effective thicknesses. The absorption spectra were obtained from the transmission measurements performed by UV-VIS-NIR spectrophotometer Shimadzu SolidSpec-3700 at room temperature. The beam diameter at the sample was in the order of a few millimeters, thus probing the average value of the molecular in-plane and out-of-plane orientation for the horizontally and vertically aligned MoS_2 layers, respectively.

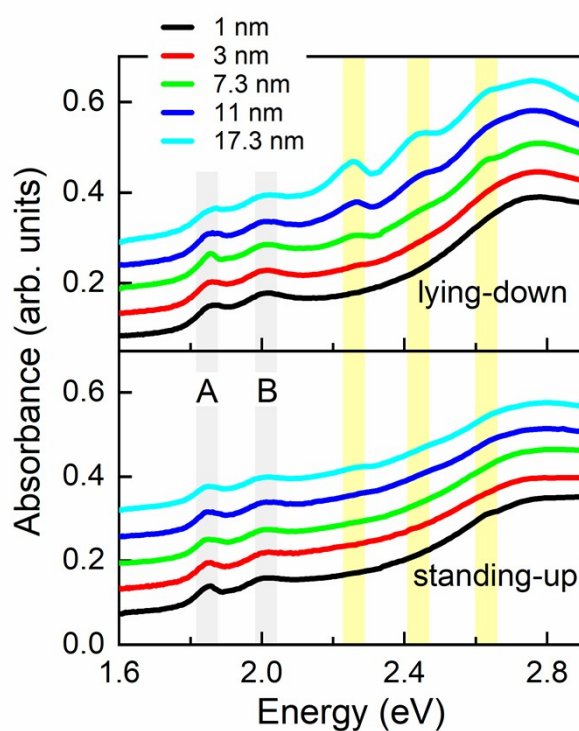


Figure S2. Absorption spectra for DIP layers with different effective thickness with lying-down and standing-up orientation of the molecules. A and B denotes the excitonic transition bands for few-layer MoS₂.² Absorption spectra are vertically shifted for clarity.

Figure S2 shows the as-measured absorption spectra for DIP layers with different effective thicknesses for the lying-down and standing-up molecules. The absorption spectra of the lying-down molecules show an increasing intensity of the transitions from the highest occupied molecular orbital (HOMO) to the lowest unoccupied molecular orbital (LUMO). For the standing-up molecules, no HOMO-LUMO transitions are visible due to a minimal projection of the polarization onto the long molecular axis. Figure S2 also shows the MoS₂ excitonic peaks A and B at 1.85 eV and 2.01 eV, respectively. The spectral position of A and B peaks agrees well with the previously published few-layer MoS₂ samples.³

3. Raman spectra

Further, we show the characteristic Raman spectra measured on DIP films. Raman spectroscopy was chosen as a complementary method to optical absorption, probing the internal vibrations of the molecules coupled to optical excitation. We measured the Raman spectra of DIP layers for both, the lying-down and standing-up orientation of molecules. The spectra were measured ex-situ using the confocal Raman spectrometer WITec alpha300 equipped with a Peltier-cooled CCD detector. The excitation laser wavelength of 785 nm (linearly polarized) was focused onto the sample by a microscope objective with a magnification of 100 \times . The excitation laser energy (1.56 eV) was chosen well below the lowest observed subband of the HOMO–LUMO transition, in order to suppress the photoluminescence (PL) background.

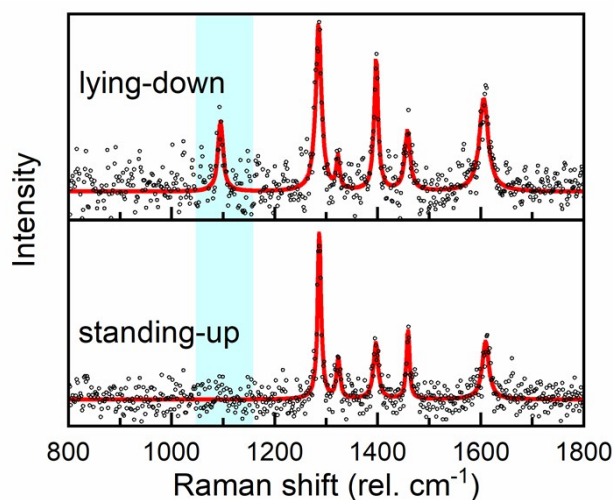


Figure S3. Raman spectra of the lying-down and standing-up orientations of DIP molecules. The effective layer thickness was 13.5 nm for both orientations. The PL background was subtracted.

The Raman spectra shown here, see Figure S3, were obtained as an average of the spectra measured in the 5 \times 5 μm^2 scanning area. Therefore, the spectra reflect the mean in-plane and

out-of-plane molecular orientation for the lying-down and standing-up molecules, respectively. We note, that in this section we would like to concentrate exclusively on the differences in the Raman spectra measured for the lying-down and standing-up molecular orientation. A detailed overview of the DIP Raman spectra, supported by the theoretical density-functional theory (DFT) calculations can be found in Ref. ⁴ and ⁵.

Figure S3 shows the Raman spectra for the two perpendicular molecular orientations. In the case of lying-down molecules, we observe a majority of the reported Raman peaks in the selected wavenumber range,⁴ which also agrees well with the theoretically calculated Raman peak positions, see Fig. S4. For the standing-up orientation of the molecules, we observed changes in the line intensity relative to the strongest line at 1284 cm⁻¹. The Raman features at ~ 1096 and 1390 cm⁻¹ are strongly suppressed. According to Ref. ⁶, all the vibrational modes from the frequency range shown in Figure S3 belong to the A_g irreducible representation of the D_{2h} point group. The corresponding Raman tensor is diagonal with three tensor elements a , b and c of uneven magnitude on the diagonal. Moreover, our DFT calculations have shown that the tensor element a is at least two orders of magnitude larger than the other two for all the modes observed in Figure S3. This means that the suppression of the 1096 and 1390 cm⁻¹ lines cannot be accounted for by rotating the Raman tensor of the mode when changing the molecule orientation from the lying-down to standing-up as the change would affect all the Raman modes of the A_g symmetry in the same manner. The line at 1096 cm⁻¹ essentially disappeared from the „standing-up“ spectrum due to its low intensity and a large background compared to the spectrum for the lying-down alignment. The reason for the suppression of the line intensity of the two Raman modes remains unknown. However, we note that similar spectral features were also observed for the DIP layers grown on SiO₂ substrate, where the molecules adopt a standing-up orientation as well.⁷

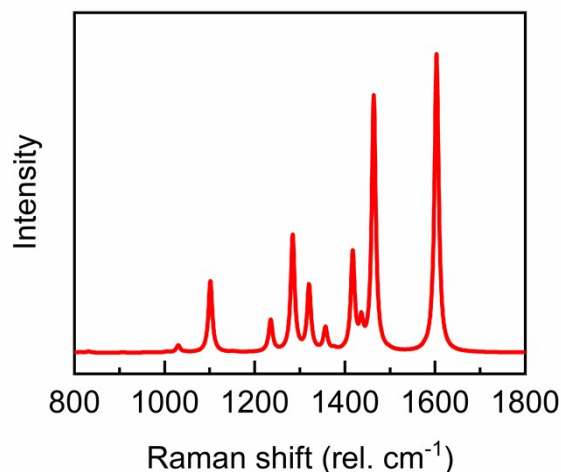


Figure S4. Raman spectrum for a single isolated DIP molecule calculated from a Hessian matrix as implemented in GAMESS package^{8,9} with use of BPW91 exchange-correlation functional and 6-31G(D, P) type of localized basis set. The calculated Raman peaks were broadened by a Lorentz function.

We also show the schematic illustration demonstrating the deflection of individual atoms for a single molecule in a gas phase for mode at 1096 cm^{-1} , see Fig. S5. The sketch was obtained from the DFT calculations and a procedure described in the figure caption of Fig. S4.

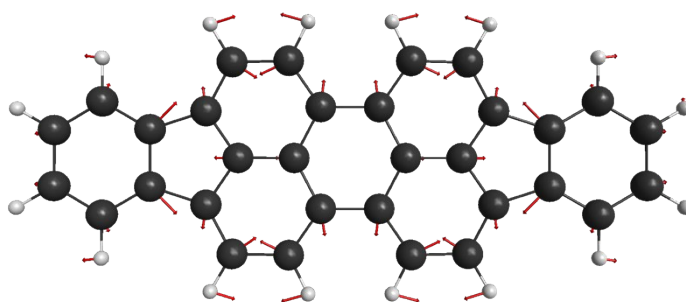


Figure S5. Deformation pattern of the Raman breathing mode at 1096 cm^{-1} obtained by the DFT calculation. The deflections of the DIP atoms are indicated by the red arrows.

References:

1. Ritley, K. A., Krause, B., Schreiber, F. & Dosch, H. A portable ultrahigh vacuum organic molecular beam deposition system for in situ x-ray diffraction measurements. *Rev. Sci. Instrum.* **72**, 1453–1457 (2001).
2. Dumcenco, D. *et al.* Large-Area Epitaxial Monolayer MoS₂. *ACS Nano* **9**, 4611–4620 (2015).
3. Mak, K. F., Lee, C., Hone, J., Shan, J. & Heinz, T. F. Atomically thin MoS₂: A new direct-gap semiconductor. *Phys. Rev. Lett.* **105**, 136805 (2010).
4. Scholz, R. *et al.* Resonant Raman spectra of diindenoperylene thin films. *J. Chem. Phys.* **134**, 014504 (2011).
5. Gisslén, L. & Scholz, R. Crystallochromy of perylene pigments: Interference between Frenkel excitons and charge-transfer states. *Phys. Rev. B* **80**, 115309 (2009).
6. Presser, V. *et al.* Raman polarization studies of highly oriented organic thin films. *J. Raman Spectrosc.* **40**, 2015–2022 (2009).
7. Zhang, D. *et al.* Plasmon resonance modulated photoluminescence and Raman spectroscopy of diindenoperylene organic semiconductor thin film. *J. Lumin.* **131**, 502–505 (2011).
8. Dykstra, C. E. *Theory and applications of computational chemistry : the first forty years.* (Elsevier, 2005).
9. Schmidt, M. W. *et al.* General atomic and molecular electronic structure system. *J. Comput. Chem.* **14**, 1347–1363 (1993).